

Florida State University Libraries

2022

Structural Determination of Kv β by Cryogenic Electron Microscopy

Vito Giovanni Evola



THE FLORIDA STATE UNIVERSITY

COLLEGE OF ARTS & SCIENCES

STRUCTURAL DETERMINATION OF Kv β
BY CRYOGENIC ELECTRON MICROSCOPY

By

Vito Giovanni Evola

A Thesis Submitted to the
Department of Biological Sciences
in partial fulfillment of the requirements for graduation with
Honors in the Major

Degree Awarded:
Summer 2022

Vito G. Evola defended this dissertation July 21, 2022.

The members of the supervisory committee were:

Dr. Scott Stagg
Thesis Director

Dr. Debra Fadool
Committee Member

Dr. Richard Bertram
Outside Committee Member

Signatures are on file with the Honors Program office

Table Contents

| | |
|----------------------|-------|
| Abstract | 4 |
| Introduction | 4-5 |
| Methods | 5-10 |
| Results & Discussion | 10-11 |
| Future Directions | 12 |
| Acknowledgements | 12 |
| Figures | 13-19 |
| References | 20-22 |

Abstract

Voltage-gated potassium (Kv) channels are tetrameric assemblies with cytosolic N- and C- termini. By attaching to a portion of the N terminus of channel polypeptides, auxiliary Kv β subunits form complexes with Kv channels (Yang, 2001). Kv β subunits have a 4:4 stoichiometry with Kv channels, but structural analyses of Kv proteins without Kv channels have revealed more than one oligomeric assembly: a tetrameric or octameric complex (Spear, 2015). Here we seek to discover a complete and coherent picture of the Kv β subunit in hopes to develop a greater understanding of how the different molecular architectures of Kv β are used to modulate Kv channel trafficking and potassium transport activities. In the present investigation, we have cloned, expressed, and purified Kv β for biochemical characterization. Additionally, the Kv β proteins have been imaged by cryogenic electron microscopy (cryo-EM) to determine the structure of the complex and characterize the tetramer/octamer equilibrium. The latter studies are ongoing. We hypothesize that the equilibrium between the octamer and tetrameric forms of Kv β and the subsequent binding to Kv channels *in vivo*, represents a new mechanism for the regulation of Kv channel activity by Kv β .

Introduction

The flow of potassium (K⁺) ions in and out of a cell, are regulated by Kv channels found within the cell membrane (Kuang, 2015). Kv channels are organized in a tetrameric form, with each monomer possessing one pore-forming domain. Collectively, each domain makes up a pore, allowing K⁺ ions to pass through (Fowler, 2013). Kv channels are important modulators of cellular excitability and have demonstrated a significant role in the maintenance of membrane potential (Shah, 2014). A variety of auxiliary subunits, termed beta subunits (Kv β) have been found and are thought to play a role in the development of functional Kv channels (Aimond, 2005). In response to adverse physiological conditions such as hypoxia and oxidative stress, Kv channels can be refined via their interactions with Kv β (Sahoo, 2014). Kv β proteins, which belong to the aldo-keto reductase (AKRs) family, catalyze the non-selective

reduction of a variety of endogenous aldehydes and ketones in the presence of NAD(P)H. These proteins participate in a range of physiological activities by coupling outward K^+ current and membrane excitability with intermediate metabolism as a function of the pyridine nucleotide redox system.

It has been demonstrated in heterologous expression systems, voltage-gated K^+ channel accessory subunits interact with the Kv-subunit monomers and affect the functionality of Kv channels (Raph, 2019). The Kv β protein has been extensively investigated with Shaker, a well-known Kv channel from *Drosophila melanogaster* (Pineda, 2008). Kv β was shown to connect with Kv channels producing the Kv channel-Kv complex soon after synthesis. The formation of this complex resulted in a 4:4 stoichiometry: four β -Kv channel subunits coupled with four α -Kv subunits (Xu, 1998). According to Gulbis, structural investigations of Kv in the absence of Kv channels revealed a structure with tetrameric C4 symmetry (1999). Furthermore, eukaryotic recombinantly produced and purified Kv was previously analyzed using negative stain electron microscopy (EM), which revealed that the protein displayed four-fold symmetry (Huizen, 1999). Those authors, however, did not undertake any additional 2D or 3D classifications, nor did they measure their particles to determine their oligomeric condition. Moreover, crystallographic structural studies of Kv β in the absence of Kv channels have yet to be performed using the full-length Kv β protein (Gulbis, 2000; Weng et al., 2006).

By overcoming earlier study restrictions, recent findings in the Stagg lab revealed that pure Kv β occurs largely as an octamer *in vitro*. In support, when expressed in the absence of additional variables, structural investigations further revealed that Kv β exists as an octameric structure with D4 symmetry (Spear, 2015). Through consideration of the expressed affinity that the tetrameric halves of the octamer have for each other the Stagg lab went on to speculate a novel regulatory mechanism by Kv β through the cycling of the octameric and tetrameric forms. On the condition that an equilibrium between different Kv β forms exists, we may have discovered a novel mechanism involved in the regulation of potassium channel activity.

Methods

Plasmid transformation

Competent DH5 α cells, acquired from the protein expression facility at Florida State University, were transformed with a pET-28a (5367bp size) expression vector containing the Kv β open reading frame (GeneBankTM accession number: EF456735). To the 50 uL of competent bacterial cells, 5 uL of pET-28a plasmid DNA was added. The mixture was cultured into 450 uL antibiotic-free liquid lysogeny broth (LB) medium and incubated at a maintained temperature of 37 °C shaking at 250 RPM for forty minutes. The competent cells were transformed by a standard heat shock method. Cells were plated on LB-agar plates supplemented with kanamycin (50 mg/mL) and chloramphenicol (34 mg/mL). These antibiotics in the same concentration were used for all cultures described here. The cultivated plates were placed in a 37 °C incubator with an atmosphere of 5% CO₂ for a period of 18-20 hours.

Plasmid DNA preparation

For each preparation, a single colony was picked with a pipette tip and transferred to a cell culture medium composed of 5mL LB treated with previously mentioned antibiotics. The culture was left to incubate in a 37 °C shaker at 250 RPM for an 18–20 hour overnight growth period. Plasmid DNA was purified using the E.Z.N.A Plasmid DNA Mini Kit I (Omega Bio-Tek). The manufacturer's instructions for the isolation of plasmid DNA from the bacterial culture was followed.

Site-Directed-Mutagenesis

QuikChangeTM kit purchased from Stratagene provided: Q5 Hot Start High-Fidelity 2X Master Mix (HF2X), Kinase-Ligase-DpnI (KLD) Enzyme Mix, KLD Reaction Buffer. All primers were synthesized by Eurofins Scientific (Forward: Kv β 418-459: 5-CTGAAAGCGTCCCTGGAGCGGCTGCAGCTGGAGTACGTGGAT; Reverse: Kv β 438-391: 5-CCGCTCCAGGGACGCTTTCAGTCCTTCAATTATGTGCTTCCTGGAAAG). PCR was performed using 1-25 ng plasmids as DNA templates in a 50 uL PCR reaction mixture containing 1uM primer pair, and one unit of Q5 High Fidelity Master Mix. The reaction started with template pre-denaturation at 98

°C for one minute, followed by thirty-five amplification cycles. Each amplification cycle consisted of 98 °C for fifteen seconds, 66 °C for thirty-seconds, and 72 °C for nine-minutes based on the length of the template construct (GeneBank™ accession number: CAA54142). The PCR cycles were finished with an extension step at 72 °C for five-minutes. 44 uL of PCR products were purified using an E.Z.N.A. Cycle pure Kit according to the manufacturer's manual. The concentration of PCR DNA was measured using a nanodrop (Thermo Scientific). The PCR products were then treated with five-units of the restriction enzyme DpnI at 37 °C for one-hour and then detected by SDS-gel electrophoresis. Digestion products were added into 50 uL DH5a competent cells by heat shock. Transformed cells inoculated to 450 uL of LB and incubated for forty-minutes maintained at 37 °C. Post-incubation, the competent cell mixture was spread on a LB-agar plate containing kanamycin and chloramphenicol and incubated overnight at 37 °C.

Individual colonies were inoculated into LB medium containing kanamycin and chloramphenicol. The inoculated LB medium was cultured at 37 °C overnight in an incubator at 250 RPM. Following overnight incubation (sixteen-hour), bacterial cells were harvested for plasmid preparation using a E.Z.N.A. Plasmid DNA Kit (Omega-Tek) following the manufacturer's manual. The concentration of the plasmids were measured using nanodrop and then verified by DNA sequencing. DNA sequencing was performed by the Florida State University sequencing facility.

Expression trials

A small-scale test expression was performed to determine the bacterial clones, medium, and the concentration of an induction reagent necessary to establish the optimal scale for large-scale growth. The following conditions were tested: bacterial clones: DH5 α , BL21, and Rosetta DE3; Medium: Lysogeny Broth and Terrific Broth (TB); Induction Reagent (IPTG): 0 mM, 50 mM, 100 mM, 500 mM, and 1000 mM. The pET-28a plasmid was transformed into each of the protein expression cell lines. To test for usable protein concentration a serial dilution for each cell line was performed in 5 mL of LB; 10⁻³, 10⁻⁴, 10⁻⁵. Each cell line dilution was plated on separate mediums treated with kanamycin and then divided into

three groups: Group A (DH5 α): [A_{1A}] 100 μ L (10^2) on 100 mm LB-agar plate; [A_{1B}] 100 μ L (10^4) on 100 mm LB-agar plate; [A_{1C}] 100 μ L (10^6) on 100 mm LB-agar plate. [A_{2A}] 100 μ L (10^2) on 100 mm TB-agar plate; [A_{2B}] 100 μ L (10^4) on 100 mm TB-agar plate; [A_{2C}] 100 μ L (10^6) on 100 mm TB-agar plate. Group B (BL21) [B_{1A}] 100 μ L (10^2) on 100 mm LB-agar plate; [B_{1B}] 100 μ L (10^4) on 100 mm LB-agar plate; [B_{1C}] 100 μ L (10^6) on 100 mm LB-agar plate. [B_{2A}] 100 μ L (10^2) on 100 mm TB-agar plate; [B_{2B}] 100 μ L (10^4) on 100 mm TB-agar plate; [B_{2C}] 100 μ L (10^6) on 100 mm TB-agar plate. Group C (Rosetta DE3) [C_{1A}] 100 μ L (10^2) on 100 mm LB-agar plate; [C_{1B}] 100 μ L (10^4) on 100 mm LB-agar plate; [C_{1C}] 100 μ L (10^6) on 100 mm LB-agar plate. [C_{2A}] 100 μ L (10^2) on 100 mm TB-agar plate; [C_{2B}] 100 μ L (10^4) on 100 mm TB-agar plate; [C_{2C}] 100 μ L (10^6) on 100 mm TB-agar plate. Five bacterial colonies were harvested from each plate and inoculated into their own separate 5 mL bath of LB treated with antibiotics. The ninety culture samples were placed in a shaking incubator maintained at 37 °C for five-hours. To test for heterologous protein expression, the varying concentrations of IPTG were added to their own solution composed of 4950 μ L of LB supplemented with antibiotics; 50 μ L of each bacterial culture were placed into their own solution followed by incubation for 14-16 hours maintained at 16 °C and 250 RPM. Samples were then prepared for and analyzed by SDS-page.

Expression and Purification of Kv β

Full-length Kv β was expressed and purified as previously reported (Weng et al., 2006; Mukhitov et al., 2016) with the following modifications: The induced culture was centrifuged at 4,000 RPM for twenty-minutes maintained at 4 °C. Bacterial cells harvested were resuspended in 30 mL lysis buffer (pH 7.5): 20 mM Tris pH 7.5, 300 mM NaCl, 1 mM MgCl₂, 10 mM imidazole, 2.5 mM of β -mercaptoethanol, supplemented with a serine protease inhibitor tablet. Cells were lysed using sonication by five two-minute burst each followed by a five-minute rest period. DNase was added to the lysate and placed on a rocker for one-hour at 4 °C. To remove waste and non-target compounds the suspension was centrifuged at 18,000 x g at 4 °C for one-hour. The supernatant was extracted while the precipitate was disposed of.

Recombinant protein was purified by passing the supernatant through a Ni²⁺-HisTrap HP 5 mL affinity column (GE Healthcare). Throughout the purification, the previously mentioned lysis buffer was utilized. Non-specifically bound proteins were removed by wash buffer: 20 mM Tris pH 7.5, 300 mM NaCl, 10 mM imidazole, 2.5 mM β -mercaptoethanol, 1 mM MgCl₂ and 1 mM ATP (loaded before use). Specifically, bound proteins were eluted by elution buffer: 20 mM Tris pH 7.5, 300 mM NaCl, 400 mM imidazole, 1 mM MgCl₂ and 2.5 mM β -mercaptoethanol. The eluted fractions were run on an SDS-gel to determine the presence and purity of full-length Kv β . Fractions containing Kv β were further purified by size exclusion chromatography (SEC). A Superose-6 SEC 10/300 25 ml column (Cytiva) was equilibrated overnight with SEC buffer: 300mM NaCl, 20mM Tris pH 7.5, and 1mM MgCl₂. Samples were pooled, concentrated, and then injected into the column. Eluted fractions were analyzed by SDS-gel. A nanodrop was used to assess the concentration of the fractions that contained the desired protein. Samples that confirmed the presence of Kv β were flash-frozen by liquid nitrogen and then stored at -80 °C

Negative Staining (EM)

After being thawed on ice, Kv β was centrifuged at 16,000 x g for 20 minutes at 4 °C to eliminate any aggregated or precipitated materials. For visualization in negative stain electron microscopy (EM), Kv β was diluted to 0.096 mg/ml using a dilution buffer (20 mM Tris pH 8.0, 150 mM KCl, 1 mM 2-mercaptoethanol). In preparation for negative staining, GC400 copper mesh grids (Electron Microscopy Sciences) were rendered hydrophilic by glow discharge in 75%/25% (v:v) Ar/O using a Solarus 950 advanced plasma system (Gatan). 3 μ l of diluted Kv β was then applied to the hydrophilic copper mesh grids. Grids were hand blotted using filter paper (Ted Pella), then immediately stained with 3 μ l of 2% Uranyl Acetate (w:v) (Electron Microscopy Sciences). Excess stain was hand blotted using filter paper and the grids were left to air dry. Before imaging, grids were kept at room temperature in a sealed desiccator. The HT7800 RuliTEM

(Hitachi) operating at 120 keV at room temperature was utilized to obtain EM micrographs of negatively stained Kv β . The equipped TVIPS camera reached a final exposure magnification of 45,000 corresponding to a nominal pixel size of 2.88 angstroms per pixel ($\text{\AA}/\text{pix}$).

Cryo-EM Data Collection and Preliminary Processing

A 5000 MWCO dialysis cassette (Thermo, USA) was used to dialyze Kv proteins overnight at 4 °C against glycerol-free buffer (20 mM Tris pH 8.0, 150 mM KCl, 1 mM beta-mercaptoethanol). Quantifoil® R2/2 200 mesh grids were made hydrophilic in the same way as described previously, and 3 μl of Kv β at 0.9 mg/ml were added to the grids. Using an FEI Vitrobot (FEI, Hillsboro OR) and the following settings: blot force = 2, blot time = 2, total blots = 1, humidity = 100%, temperature = 4 °C, grids were vitrified in liquid nitrogen-cooled ethane. Movie frames were collected using Leginon for automated data acquisition on a Titan Krios equipped with a Direct Electron Apollo detector at 75,000 magnification, super-resolution mode with a pixel size of 0.58 \AA .

Results & Discussion

Plasmid Transformation

The abundant presence of single bacterial colonies on LB-agar plates shows that the transformation of the pET-28a into DH5a E. Coli cells was successful.

Site-Directed Mutagenesis

DNA sequencing revealed a mutation in the pET-28a containing plasmid Kv β . A tyrosine in place of a serine amino acid resulted in an early truncation of the desired Kv β protein (Figure 1). To combat the mutation, we performed site-directed mutagenesis. Mutagenesis was deemed successful after sequencing our mutated DNA product and comparing the sequence to a control sequence found on the BLAST database.

Expression & Purification

We found that *E. Coli* cells containing Kv β could be optimally grown on LB-agar plates treated with both Chloramphenicol and Kanamycin. Further, we discovered that Kv β could be optimally expressed when treated with 50mM of IPTG. Interestingly, we observed that at higher concentrations of IPTG, Kv β was observed to be toxic leading to the degradation of other proteins present within the cell (Figure 2). Post induction samples confirmed Kv β migrates as a ~ 35 – 40 kDa monomer as seen by 12% sodium dodecyl sulfate-polyacrylamide gel electrophoresis (SDS-PAGE) analysis (Figure 3). This confirms Kv β was successfully expressed. Following the expression, purification by nickel-column NTA chromatography showed Kv β eluted at a volume of 150 – 200 ml (Figure 4). The SEC chromatogram showed three peaks each of which was run on an SDS-gel and confirmed the presence of Kv β (Figure 5).

Negative Staining

Purified protein fractions containing Kv β were obtained from SEC. Upon visualization using an electron microscope (EM), negatively stained copper grids showed small homogenous and monodispersed particles (Figure 6). This demonstrated that Kv β forms discrete well-ordered particles in solution that are not aggregated. These particles contain a central channel that is surrounded by radiating density.

Cryo-EM

9,372 images of ice embedded, full-length Kv β (Figure 7) were collected. These revealed that the specimen survived plunge-freezing intact, and the Kv β oligomers remain in the octameric state. CTF was estimated, and the resolution went out to 0.58 Å on average indicating that the dataset has the potential to go to high resolution during the single particle reconstruction stage. It is anticipated that we will be able to achieve a near-atomic resolution reconstruction of the specimen in the future processing steps.

Future Directions

Single Particle Analysis

A number of processing steps remain before determining the Kv β structure. The first steps will be to align the movie frames, estimate the CTF, and pick particles using the Appion processing suite (Lander et al. 2009). Following that, two-dimensional and three-dimensional classifications will be performed using a maximum likelihood alignment algorithm in Relion. After classification, particles will be selected for final refinement and reconstruction.

Atomic Modeling

A homology model of Kv β will be constructed in MobWeb. When constructed, the homology model will be compared and aligned in UCSF Chimera (Pettersen et al., 2004) using the MatchMaker function. To generate an octameric complex model, the model will be subjected to D4 symmetry. The homology model will be rigid fit to a density map using the fit function in UCSF Chimera and the final model will be flexibly fitted to a density map running Molecular Dynamics Flexible Fitting (MDFF) (Trabuco et al., 2008).

Acknowledgments

I want to thank the Stagg Lab for everything they have taught me this past year. Firstly, I want to thank Ruizhi (Ray) for being my mentor during the entirety of my research project. Thank you to Ananya for her continuous assistance and support during times of confusion. And lastly, I am especially thankful to Dr. Stagg for the given opportunity to conduct research in his lab. A special thanks to Anandi for being my desk-buddy.

Figure 1

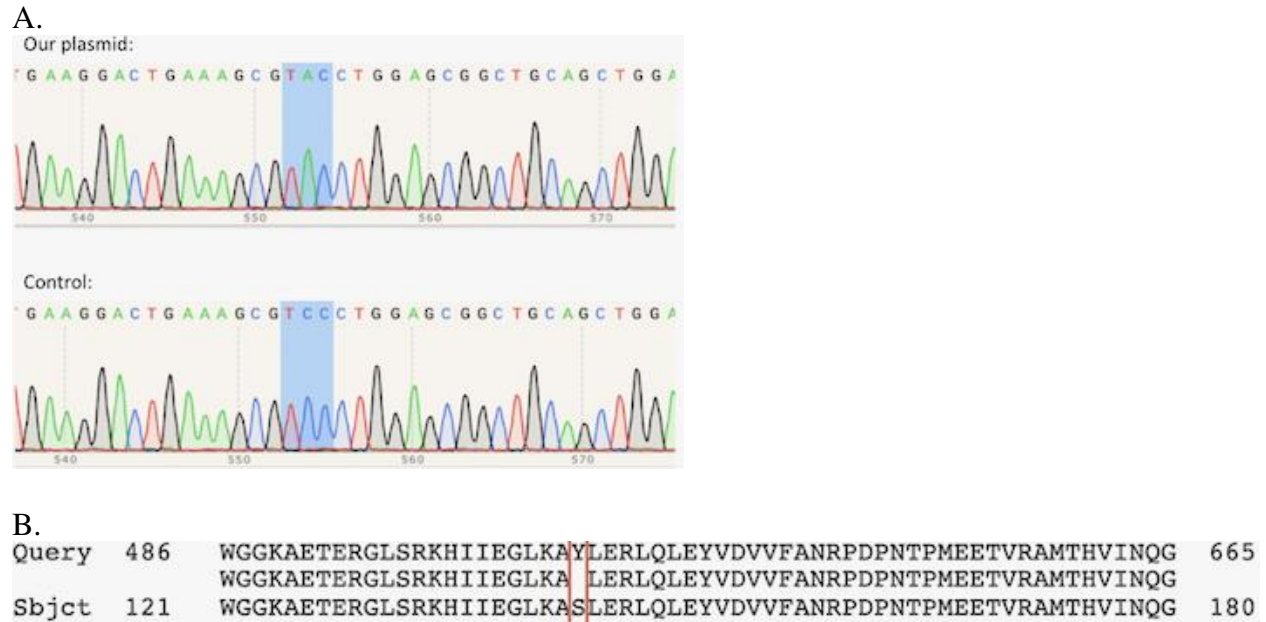


Figure 1: Identification of the single-point mutation (A) and location of the altered amino acid (B).

Figure 2: The pET-28a plasmid DNA was sequenced and compared to a control found on the BLAST data base. Control sequence contained a serine residue at position 508 whereas our plasmid sequence contained a tyrosine group. Adenine to cytosine mutation was desired and achieved.

Figure 2

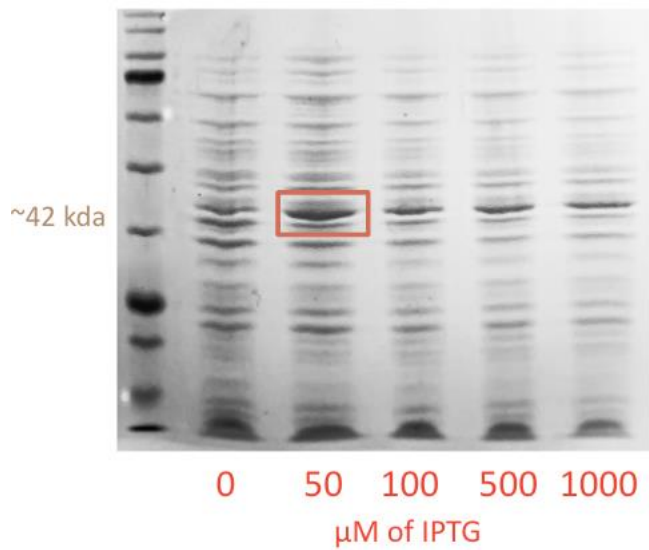


Figure 2: SDS-gel presenting K $\nu\beta$ post induction optimization trials.

Figure 2: K $\nu\beta$ appears at 42kda on an SDS-gel. The induction of K $\nu\beta$ was optimal when treated with 50 μM of IPTG. It appears that at higher concentrations of IPTG K $\nu\beta$ was toxic to other cellular proteins. This is suggested by the decreased intensity of bands peripheral to the band identifying K $\nu\beta$.

Figure 3

A.

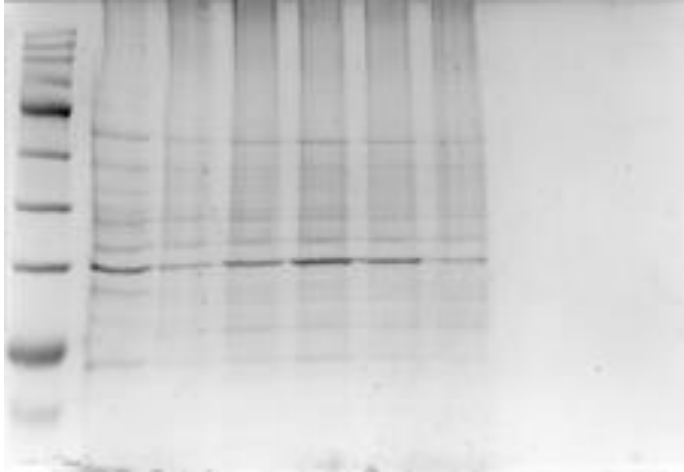
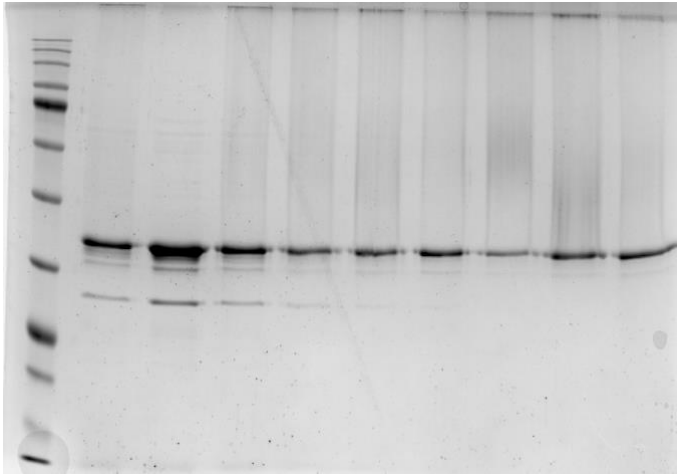


Figure 3: Post-Induction of K ν β with 50 μ M of IPTG.

Figure 3: Induction of K ν β was successful as demonstrated by the consistency of bands located at 42kda across each sample.

Figure 4

A.



B.

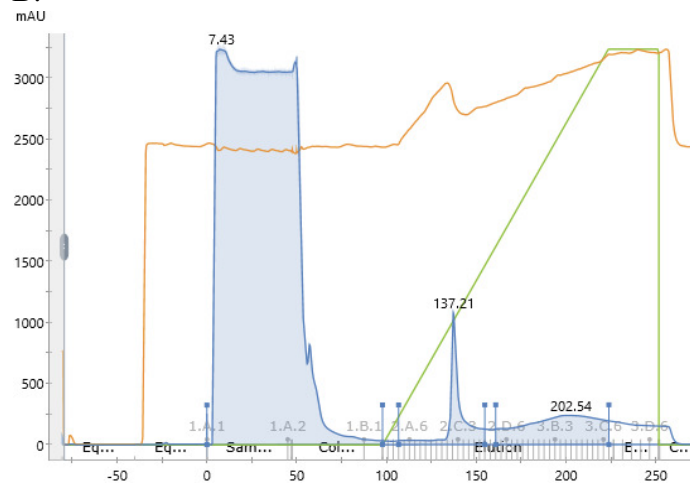
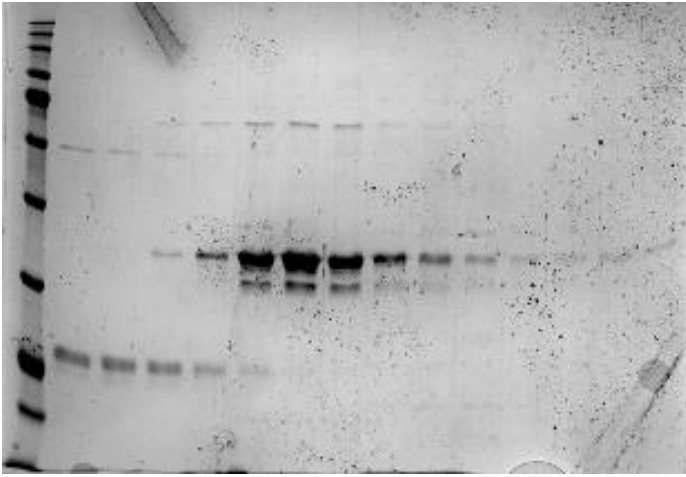


Figure 4: SDS-gel post-purification by nickel-column chromatography (A). Chromatogram containing several peaks representing wash, junk, and Kv β respectively.

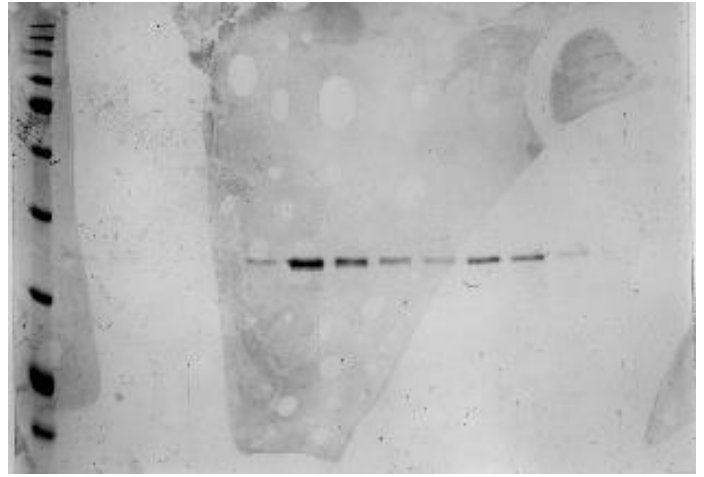
Figure 4: Purification by nickel-column chromatography shows peaks around 60 ml, 140 ml, and 200 ml. Kv β was successfully isolated from other cellular components.

Figure 5

A.



B.



C.

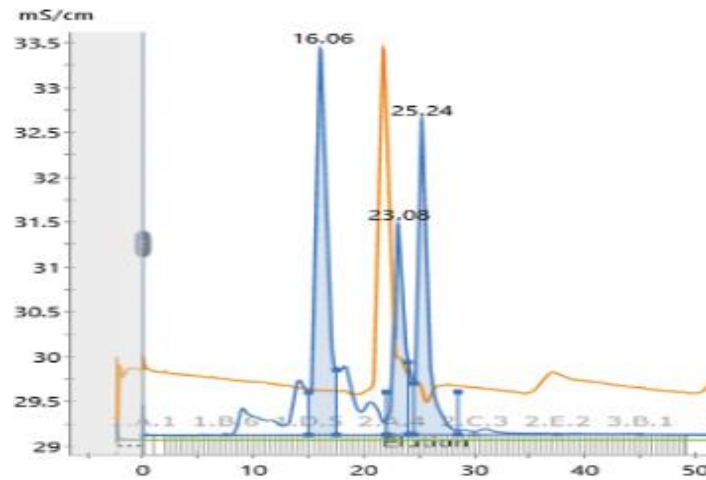
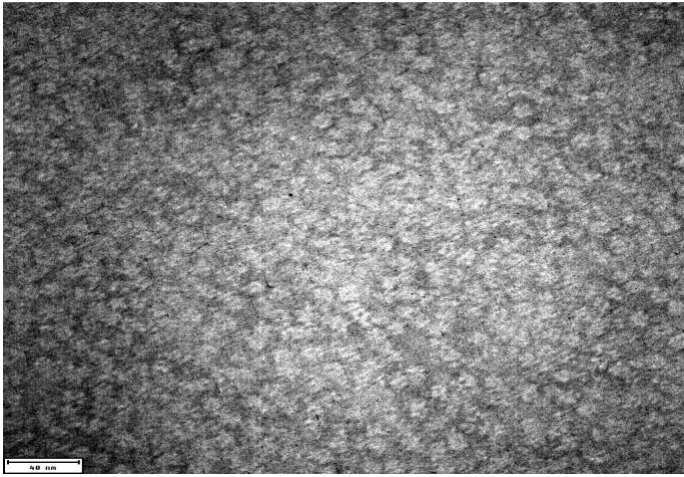


Figure 5: Samples were pooled following SEC and purity evaluated by SDS-gels (A & B). A three peak chromatogram representing the SEC results.

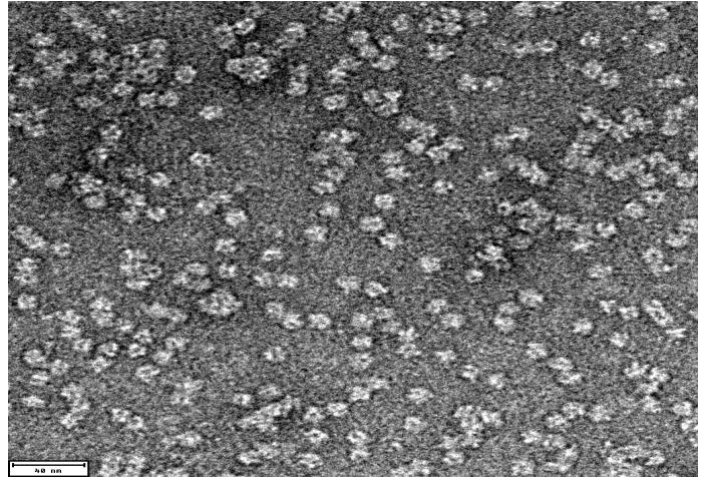
Figure 5: Band intensity indicated an ideal concentration of Kv β . SEC results provided three peaks. The first appeared around 16 mL, representing the octameric structure of Kv β . The second and third peak peak appeared at 140 mL and 200 mL respectively and pertains to the monomeric structure of Kv Kv β .

Figure 6

A.



B.



C.



Figure 6: Images taken on the Electron Microscope. Image A corresponds to the first peak present on the SEC chromatogram. While image B and C represent the remaining peaks respectively.

Figure 6: Each image presents a different concentration of protein particles containing a central channel surrounded by radiating density ($K\alpha\beta$). Evaluation of protein samples showed an optimal concentration that could later be evaluated via Cryo-EM.

Figure 7

A.

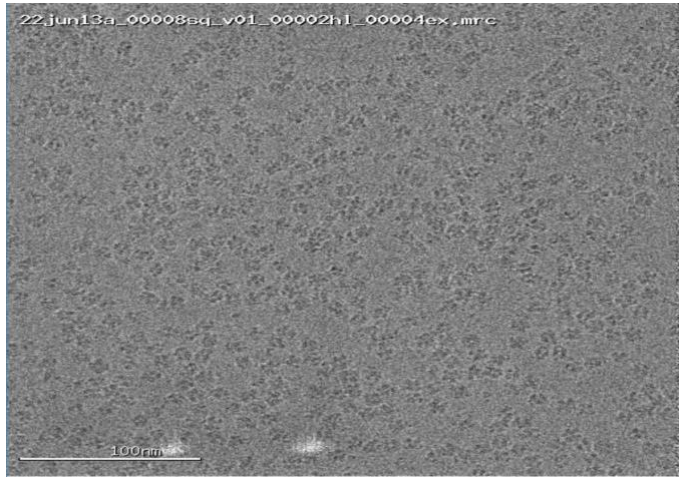


Figure 7: Image taken via Cryo-EM on the Titan Krios (A).

Figure 7: Data collection took place on the Titan Krios and image shows monodispersed particles of Kv β . Like the results from negative stain, image presents a central channel with radiating density. Concentration of Kv β appears optimal.

References

- Aimond, F., Kwak, S. P., Rhodes, K. J., & Nerbonne, J. M. (2005). Accessory Kv β_1 subunits differentially modulate the functional expression of voltage-gated K $^+$ channels in mouse ventricular myocytes. *Circulation Research*, *96*, 451-458.
<https://doi.org/10.1161/01.RES.0000156890.25876.63>
- Fowler, P. W., & Sansom, M. S. P. (2013). The pore of voltage-gated potassium ion channels is strained when closed. *Nature Communications*, *4*, 1872. <https://doi.org/10.1038/ncomms2858>
- Gulbis, J. M., Mann, S., & Mackinnon, R. (1999). Structure of a voltage-dependent K $^+$ channel β subunit. *Cell*, *97*(7), 943-952. [https://doi.org/10.1016/S0092-8674\(00\)80805-3](https://doi.org/10.1016/S0092-8674(00)80805-3)
- Huizen, R. V., Czajkowsky, D. M., Shi, D., Shao, Z., Li, M. (1999). Images of oligometric Kv β_2 , a modulatory subunit of potassium channels. *FEBS Letters*, *457*(1), 107-111. [https://doi-org.proxy.lib.fsu.edu/10.1016/S0014-5793\(99\)01021-2](https://doi-org.proxy.lib.fsu.edu/10.1016/S0014-5793(99)01021-2)
- Kuang, Q., Purhonen, P., & Hebert, H. (2015). Structure of potassium channels. *Cellular and Molecular Life Science*, *72*, 3677-3693. <https://doi.org/10.1007/s00018-015-1948-5>
- Lander, G. C., Stagg, S. M., Voss, N. R., Cheng, A., Fellmann, D., Pulokas, J., Yoshioka, C., Irving, C., Mulder, A., Lau, P.-W., Lyumkis, D., Potter, C. S. & Carragher, B. (2009). Appion: an integrated, database-driven pipeline to facilitate EM image processing. *J Struct Biol*, *166*(1), 95-102. <https://doi.org/10.1016/j.jsb.2009.01.002>

- Pettersen, E. F., Goddard, T. D., Huang, C. C., Couch, G. S., Greenblatt, D. M., Meng, E. C. & Ferrin, T. E. (2004). UCSF chimera – a visualization system for exploratory research and analysis. *J Comput Chem*, 25(13), 1605-12. <https://doi.org/10.1002/jcc.20084>
- Pineda, R. H., Knoeckel, C. S., Taylor, A. D., Estrada-Bernal, A., Ribera, A. B. (2008). Kv1 Potassium channel complexes in vivo require Kv β 2 subunits in dorsal spinal neurons. *Journal of Neurophysiology*, 100(4), 2125-2136. <https://doi.org/10.1152/jn.90667.2008>
- Raph, S. M., Bhandnagar, A., & Nystoriak, M. A. (2019). Biochemical and physiological properties of K⁺ channel-associated AKR6A (Kv β) proteins. *Chem Biol Interact*, 305, 21-27. <https://doi.org/10.1016/j.cbi.2019.03.023>
- Sahoo, N., Hoshi, T., & Heinemann, S. H. (2014). Oxidative modulation of voltage-gated potassium channels. *Antioxidants & Redox Signaling*, 21(6), 933-952. <https://doi.org/10.1089/ars.2013.5614>
- Shah, N. H., & Aizenman, E. (2014). Voltage-gated potassium channels at the crossroads of neuronal function, ischemic tolerance, and neurodegeneration. *Trans Stroke Res*, 5(1), 38-58. <https://doi.org/10.1007/s12975-013-0297-7>
- Spear, J. M. (2015). Early secretory mechanism and progress toward structural determination of the voltage-gated potassium channel Kv1.3. Florida State University, Institute of Molecular Biophysics.
- Trabuco, L. G., Villa, E., Mitra, K., Frank, J., Schulten, K. (2008). Flexible fitting of atomic structures into electron microscopy maps using molecular dynamics. *Structure*, 16(5), 673-83. <https://doi.org/10.1016/j.str.2008.03.005>

Weng, J., Cao, Y., Moss, N., Zhou, M. (2006). Modulation of voltage-dependent shaker family potassium channels by an aldo-keto reductase. *J Biol Chem*, 281(22), 15194-200.
<https://doi.org/10.1074/jbc.M513809200>

Xu, J., Yu, W., Wright, J. M., Raab, R. W., Li, M. (1998). Distinct functional stoichiometry of potassium channel beta subunits. *Proc Natl Acad Sci USA*, 95(4), 1846-51.
<https://doi.org/10.1073/pnas.95.4.1846>